ANS UV observations of external galaxies. II - UV photometry of M 31, M 33, M 81, M 101, NGC 2403 and several Zwicky galaxies

Israel, F.P.; Boer, K.S. de; Bosma, A.

ASTRONOMY & ASTROPHYSICS
SUPPLEMENT SERIES

Astron. Astrophys. Suppl. Ser. **66,** 117-130 (1986)

ANS UV observations of external galaxies. II. UV photometry of M 31, M 33, M 81, M 101, NGC 2403 and several Zwicky galaxies.

F. P. Israel ([1]), K. S. de Boer ([2]), and A. Bosma ([3])

([1]) Astronomy Division, Space Science Department, European Space Agency (ESA), Estec, 2200 AG Noordwijk, The Netherlands
([2]) Kapteyn Astronomical Institute, Groningen, The Netherlands (*)
([3]) Sterrewacht, Huygens Laboratorium, 2300 RA Leiden, The Netherlands

Received March 27, accepted November 18, 1985

Summary. — Five-colour area-integrated UV photometric results are given of 2.5 × 2.5 arcmin fields in the galaxies M 31, M 33, M 81, M 101 and NGC 2403. Most of these fields are centred on bright HII regions. The UV fluxes detected are generally representative of OB associations. The data for the nearby galaxies indicate radial gradients in brightness and colour within these galaxies. In addition, results are presented of a survey of Zwicky-type dwarf galaxies.

Key words : UV observations — galaxies — area-integrated photometry.

1. Introduction.

Because of their sensitivity to the emission of bright early-type stars, UV observations of galaxies are of great importance for our understanding of the young stellar population in galaxies. Especially when combined with visual and infrared observations that contain mainly information on stars of later type valuable insight can be gained on overall galaxy parameters in particular as a function of Hubble type. For this reason, several galaxies of widely varying types were observed by the Groningen University UV experiment on board of the Astronomical Netherlands Satellite ANS. Most of the results of this survey have been published in the ANS catalogue (Wesselius *et al.*, 1982). Aspects of the data on M 31, M 81 and some other galaxies have been discussed by Wu *et al.* (1980) and Coleman *et al.* (1980), while data on elliptical galaxies, including the M 31 companions were presented by de Boer (1982). Results on part of the LMC, including several HII regions in the 30 Doradus region have been discussed by Koornneef (1977) and Israel and Koornneef (1979, Paper I).

In this paper we present the detailed observations of the Local Group galaxies M 31 and M 33, and the well-studied nearby galaxies M 81 and M 101 not contained in the ANS catalogue. We also present the results of a survey of (weak) Zwicky-type dwarf galaxies, in which only four were detected with the ANS. Further analysis of the observations in this paper is in preparation.

2. Observations.

The ANS was launched in August, 1974 and was in operation for a period of about one and a half year. The Groningen University UV experiment consisted of a 22 cm telescope and a five-channel photometer operating at wavelengths of 1550, 1800, 2200, 2500, 3300 Ångströms. The photometer had a 2.5 × 2.5 arcmin square aperture. Pointing was maintained with an accuracy of 20 arcsec or better by tracking a bright $\left(m_V < 8^m\right)$ field star (see de Boer and van Albada, 1976). A full description of the instrument and its operation is given by Wesselius *et al.* (1982). We generally used the standard ANS reduction procedures to obtain corrected counts per second for each field. The correction includes the effect of a drift in photometer sensitivity (Wesselius *et al.*, 1982). Since the photometry of galaxies yields only very low count rates, it is of the outmost importance to have a good calibration of the dark current and blank sky count rates. For the ANS automated reduction, these values were determined from data randomly distributed over the sky. Here we use the carefully determined blank sky and dark current countrates determined by Koornneef and de Boer (1975) from preselected star-free fields at high galactic latitudes outside the zodiacal light. These fields were generally not near the objects observed. However, use of the derived corrections on fields expected to be empty near the observed galaxies yield, within the errors, consistent results. These correction factors

(*) Postal Address : Royal Greenwich Observatory, Herstmonceux (E.S.).
Send offprint requests to : F. P. Israël.

differ somewhat from those found by Koornneef (private communication) in his study of the LMC. Table I lists the difference between our calibration and the standard ANS calibration to allow the judgement of its effect on the galaxy photometry. Counts were converted to flux-densities following the absolute calibration given by Wesselius *et al.* (1980). Usually, fields were observed more than once ; we determined errors by the repeatability of individual integrations. The errors thus determined correspond to about 2 σ r.m.s. The 2200 Ångström band had greatest sensitivity, followed by the 1800 and 2500 Ångström bands. Data in the 3300 Ångström band were frequently contaminated with background noise due to the radiation environment of the satellite. When this was the case, we have either ignored the observation or determined an upper limit.

The resulting flux densities for each field are given in tables II through VII ; the position of each field is also given in the tables, and for M 31, M 33, M 81 and M 101 is indicated in figures 1 through 4.

3. Results.

3.1 M 31 (NGC 224). — The ANS observations of M 31 (Sb I) and surroundings fall into four categories : (i) OB associations in the NE spiral arm (12 fields) ; (ii) OB associations in the SW spiral arm (19 fields) ; (iii) the central part (5 fields) and (iv) the companions NGC 205 and NGC 221 (8 fields). The latter have been discussed by de Boer (1982) and will not be dealt with further, except by noting that the UV intensities of NGC 221 resemble those of elliptical galaxies, whereas those of NGC 205 resemble those of blue globular clusters. We also note that observations of the nucleus of M 31 were discussed by Wu *et al.* (1980). The NE and SW spiral arm regions observed coincide with regions of relatively strong radio continuum emission with a relatively flat spectrum (see Beck and Gräve, 1982) suggesting the presence of a significant thermal component. They also correspond to the regions of strongest far-infrared (see Habing *et al.*, 1984) and strongest UV (2000 Å) emission as can be seen in the balloon UV image obtained by Deharveng *et al.* (1980).

In figure 5 we show the mean UV spectrum for each category. The NE arm OB associations generally appear to have a somewhat higher late-type stellar contribution than the SW arm OB associations. This probably is a consequence of the location of the observed NE fields near the minor axis. The large tilt of M 31 then causes the sampling of a relatively large interval in radial distance to the center of M 31. Both arm regions show a pronounced difference with the central region which is dominated by evolved stars. A comparison of the present results can be made with the data obtained by Deharveng *et al.* (1980). For the central region they find an integrated flux density $F_{1990} = 4.7 \pm 2.0 \times 10^{-13}$ erg cm^{-2} s^{-1} Å^{-1} and for OB 78 (NGC 206) a value $F_{1990} = 3.0 \pm 1.3 \times 10^{-13}$ erg cm^{-2} s^{-1} Å^{-1}. For the same regions we infer from our data values of respectively $3.8 \pm 0.3 \times 10^{-13}$ and $2.3 \pm 0.1 \times 10^{-13}$ erg.cm^{-2} s^{-1} Å^{-1} which is in very good agreement. Finally we note that the contrast between the central region and the spiral arm regions decreases rapidly with increasing wavelength. The surface brightness in the central region (at $R = 5'$) is about a factor of 30 higher than in the arms (at $R = 60'$) in both the B band (Hodge and Kennicutt, 1982) and at 3300 Å. At 2200-2500 Å the difference has decreased to a factor of about 3, and at 1550-1880 Å it is only about a factor of 1.6. This behaviour is also clearly shown in the UV and *UBV* profile of M 31 published by Davis *et al.* (1982).

3.2 M 33 (NGC 598). — The Sc III spiral M 33 was covered extensively, with emphasis on the spiral arms and bright HII regions. A few fields are contaminated by galactic foreground stars. The case of an 11th magnitude early A star in the field of NGC 604 was discussed by Israël *et al.* (1982). The worst case is that of field # 19 which has been rendered useless by what appears to be an 8th magnitude A5-A6 star with reddening $E(B\text{-}V) = 0.05$. Only at 1550 Å there appears to be a noticeable contribution due to M 33. Inspection of visual images of M 33 suggests possible contamination of fields ## 2, 3, 40 and 41 by stars of 13th to 14th magnitude. However, only the UV spectra of fields ## 2 and 41 show a significant rise at 3300 Å so that we expect the influence of this contamination at the shortest wavelengths to be small.

Only a few HII region fields contain ionizing OB clusters bright enough to provide sufficient contrast with their surroundings. The clearest case is that of NGC 604 (Israël *et al.*, 1982). Careful comparison with nearby fields shows significant flux density excesses for the fields containing the HII regions IC 133, IC 131, NGC 592, IK 25, IK 53 and perhaps IK 44 (cf. Israël and van der Kruit, 1973). At our resolution of 2.5 arcmin, the second brightest HII region NGC 595 is difficult to separate from the relatively intense emission of the central part of M 33.

The galaxy was sufficiently well covered to enable us to determine the overall distribution of UV emission as a function of radius. Three effects are noticeable. Firstly, at all wavelengths the UV surface brightness decreases monotonically as a function of radius. Secondly, the UV emission becomes bluer with increasing radius. Davis *et al.* (1982) already noted, in a similar way, that the spiral arms of M 33 are significantly bluer than the nucleus. Both these effects are shown in figure 6, where we have plotted all observed flux densities as a function of wavelength and radius. The parameters of the linear regression fits to these data are given in table VIII. Subtraction of the extrapolated flux densities at $R = 0$ from the actually observed values yields the « bulge excess » spectrum shown in figure 7. Figure 8 combines the present UV data for the center of M 33 with optical flux densities derived from Guidoni *et al.* (1981). We have also included the S2/68 UV results for the 9×9 arcmin central region, and the UV flux densities integrated over roughly 25×45 arcmin (Carnochan *et al.*, 1979). To the latter we have added the *UBV* flux densities from de Vaucouleurs *et al.* (1976). As the optical size defined by these authors is much larger than

the area over which Carnochan *et al.* (1979) have integrated their UV flux densities, the latter may have been underestimated with respect to the optical values possibly causing the sharp rise between λ2740 Å and λ3650 Å. Thirdly, the 2200 Å dip is most noticeable for the spectra between $R = 1$ kpc and $R = 3$ kpc. Interpretation of these results is deferred to a following paper.

3.3 M 81 (NGC 3031). — The Sb I galaxy M 81 was completely covered, but at almost all positions the UV signal was very weak and close to the noise. An exception to this is the nuclear bulge of M 81, which is very strong, especially at the longest observed wavelengths, and has a UV spectrum very similar to that of the central bulge of M 31 (see Wu *et al.*, 1980). In figure 9 we show flux densities in the three most sensitive ANS channels (λλ1800, 2200 and 2500 Å) as a function of radius. In figure 10 we show the same, but now averaged over one arcmin bins. Optical surface brightness profiles along the major axis (Guidoni *et al.*, 1981) show a strong radial dependence, with a scale length of about 5 arcmin in the *U* band. The UV data in figures 9 and 10 are expected to show only a smoothed gradient, because a) data are included from all measured positions, b) the aperture is relatively large compared to the size of M 81 and c) M 81 has a large inclination. Nevertheless, our photometry shows a radial gradient at λ2200 Å, possibly a weak gradient at λ2500 Å, and an essentially flat surface brightness distribution at λ1800 Å. Indeed, UV spectra averaged over two-arcmin radial intervals (not shown) indicate λ2200 Å absorption strengths to increase with radius. The optical data by Guidoni *et al.* (1981) in addition show peaks at 5.8, 9.0 and 12.5 arcmin from the nucleus ; the first two gain in prominence towards shorter wavelengths and can be recognized in the UV data as well. They reflect the presence of concentrations of young and luminous stars in the spiral arms. The outer peak loses its prominence towards shorter wavelengths, and is not covered by our UV data.

3.4 M 101 (NGC 5457). — Balloon- and rocket-borne UV images of M 101 at λ2000 and at λ2250 Å were obtained by Donas *et al.* (1981), Stecher *et al.* (1982) and Hill *et al.* (1984). In particular the results of the latter show the UV surface brightness distribution of the galaxy to be dominated by the spiral arms, with clear maxima coinciding with the giant HII region complexes. As figure 4 shows, we did not cover the whole galaxy, but obtained measurements mainly of the southeastern half of M 101, with emphasis on the giant HII region complexes. UV results on these HII region complexes were discussed by Blitz *et al.* (1981). The measured UV surface brightness is generally higher than in M 31 and M 81, and comparable to that measured in M 33. UV spectra of M 101 are shown in figure 11. In order to improve the signal-to-noise ratio, we have averaged over different subsets of the data. Figure 11a shows the mean spectrum of all observed positions, with a clear λ2200 Å feature. This feature is only weakly seen in the mean HII region UV spectrum (Fig. 11b ; cf. Blitz *et al.*, 1981). Interestingly, it is again clearly present in figure 11c which shows the mean UV spectrum of positions in the South-Eastern half of M 101 adjacent to, but not coinciding with the giant HII region complexes. Since the HII region complexes of M 101 are generally smaller than the ANS 2.5 arcmin square aperture, the spectrum in figure 11b will be contaminated by emission from blue stars outside their boundaries. In order to gauge the effect of this contamination, figure 11d shows the difference spectrum of figures 11b and 11c. To within the errors, there is now no sign of a λ2200 Å absorption feature in the HII regions at all. Finally, figure 11e shows the mean spectrum of the three positions observed in the North-Western half of M 101, which is devoid of giant HII region complexes. Contrary to the other spectra which are characteristic of early type (OB) stars with some amount of extinction, the spectrum in figure 11e appears to be more heavily influenced by later type (A) stars. Flux densities as a function of radial position in M 101 are given in figure 12. The results of linear regression fits on these data are given in table IX. Although the evidence is not strong, the same pattern as in M 33 emerges : weak gradients in the total surface brightness of M101 appear to be present at all observed wavelengths, and the M 101 colours tend to be bluer towards the edges of the galaxy. One should bear in mind, however, that these results mostly refer to the southeastern half of M 101. Comparison with the analysis of Hill *et al.* (1984) shows that the colour gradient in M 101 is mostly due to the spiral arm emission rather than to the disk emission.

3.5 NGC 2403. — In the large, nearby Sc III galaxy NGC 2403 (which is a member of the M 81 group) only three positions were observed : the nucleus, and two positions coinciding with the brightest HII region complexes VS 44 and VS 41 (cf. Israël, 1980). All three UV spectra are characteristic of a dominant OB star population, contaminated mainly at the longest wavelength (3300 Å) by stars of later type.

3.6 COMPACT (ZWICKY) GALAXIES. — We observed 28 galaxies from Zwicky's lists for 22 of which Sargent (1970) had obtained optical spectra. Only four objects (VIIZw16 = NGC 1569, IIIZw59 = NGC 2595, IIZw47 and VIIZw511 = NGC 5144) were clearly detected while three more were detected at the threshold level (IIZw53, VIIZw490 and IZw18 — which has the overall characteristics of a giant extragalactic HII region ; cf. Sargent and Searle, 1970). The UV spectra of all four clearly detected objects are characteristic of slightly reddened OB associations. The results on NGC 1569 (not tabulated) will be dealt elsewhere ; at λ3300 Å the UV measurements are strongly contaminated by the galactic foregound GO star BD + 64451 $\left(m_p = 10.0 \text{ mag}\right)$. In the direction of IZw26 (not tabulated) we detected a strong signal which turned out to be due to the galactic F0 star BD + 551461 $\left(m_V = 8.2 \text{ mag}\right)$. From our detection statistics we infer that the limiting magnitude of the ANS UV instrument for this type of galaxy was about $m_V = 15.5$.

Acknowledgements.

We thank the members of the ANS team, in particular P. R. Wesselius and A. R. W. de Jonge for their efforts in obtaining the data, and for help and advice in the reduction stages. The ANS was sponsored by the Geophysics and Space Research Committee of the Royal Netherlands Academy of Sciences (KNAW).

References

BECK, R., GRÄVE, R. :1982, *Astron. Astrophys.* **105,** 192.
BLITZ, L., ISRAËL, F. P., NEUGEBAUER, G., GATLEY, I., LEE, T. J., BEATTIE, D. H. : 1981, *Astrophys. J.* **249,** 76.
CARNOCHAN, P. J., NANDY, K., MORGAN, D. H. : 1979, *Mon. Not. R. Astron. Soc.* **187,** 763.
COLEMAN, G. D., WU, C. C., WEEDMAN, D. W. : 1980, *Astrophys. J. Suppl. Ser.* **43,** 393.
DE BOER, K. S. : 1982, *Astron. Astrophys. Suppl. Ser.* **50,** 247.
DE BOER, K. S., VAN ALBADA, T. S. : 1976, *Astron. Astrophys.* **52,** 59.
DAVIS, J., CODE, A. D., MATHIS, J. S., WELCH, G. A., : 1982, *Astron. J.* **87,** 849.
DEHARVENG, J. M., JAKOBSEN, P., MILLIARD, B., LAGET, M. : 1980, *Astron. Astrophys.* **88,** 52.
DONAS, J., MILLIARD, B., LAGET, M., DEHARVENG, J. M. : 1981, *Astron. Astrophys.* **97,** L7.
GUIDONI, U., MESSI, R., NATELI, G. : 1981, *Astron. Astrophys.* **96,** 215.
HABING, H. J. *et al.* : 1984, *Astrophys. J. Lett.* **278,** L59.
HILL, J. K., BOHLIN, R. C., STECHER, Th. P. : 1984, *Astrophys. J.* **247,** 542.
HODGE, P. W., KENNICUTT, R. C. : 1982, *Astron. J.* **87,** 264.
ISRAËL, F. P. : 1980, *Astron. Astrophys.* **90,** 246.
ISRAËL, F. P., GATLEY, I., MATTHEWS, K., NEUGEBAUER, G. : 1982, *Astron. Astrophys.* **105,** 229.
ISRAËL, F. P., KOORNNEEF, J. : 1979, (Paper I), *Astrophys. J.* **230,** 390.
ISRAËL, F. P., VAN DER KRUIT, P. C. : 1973, *Astron. Astrophys.* **32,** 363.
DE JONGE, A. R. W. : 1979, ROG Internal Note ROG 79-39.
KOORNNEEF, J. : 1977, *Astron. Astrophys. Suppl. Ser.* **29,** 117.
KOORNNEEF, J., DE BOER, K. S. : 1975, ROG Internal Note ROG 75-63.
SARGENT, W. L. W. : 1970, *Astrophys. J.* **160,** 405.
SARGENT, W. L. W., SEARLE, L. : 1970, *Astrophys. J. Lett.* **162,** L155.
STECHER, T. P., BOHLIN, R. C., HILL, J. K., JURA, M. A. : 1982, *Astrophys. J. Lett.* **255,** L99.
DE VAUCOULEURS, G., DE VAUCOULEURS, A., CORWIN, H. C. : 1976, « Second Reference Catalog of bright Galaxies » (Univ. of Texas Press, Austin).
WESSELIUS, P. R., VAN DUINEN, R. J., DE JONGE, A. R. W., AALDERS, J. W. G., LUINGE, W., WILDEMAN, K. J. : 1982, *Astron. Astrophys. Suppl. Ser.* **49,** 427.
WESSELIUS, P. R., VAN DUINEN, R. J., AALDERS, J. W. G., KESTER, D. : 1980, *Astron. Astrophys.* **85,** 221.
WU, C. C., FABER, S. M., GALLAGHER, J. S., PECK, M., TINSLEY, B. M. : 1980, *Astrophys. J.* **237,** 290.

TABLE I. — *Effect of improved dark-current/blank sky correction on UV fluxesfor high-latitude galaxies in* 10^{-14} erg cm^{-2} s^{-1} Å^{-1}.

Wavelength (A)	1550Å	1800Å	2200Å	2500Å	3300Å
F (Standard) - F (This Paper)	-2.65	-3.11	-0.73	-0.94	-1.23
Dispersion in 'Standard'	+0.41	+1.84	+0.78	+1.88	+3.23
Calibration					

Note : « Standard » refers to dark-curent/blank sky corrections used in the standard ANS automated reduction procedure (de Jonge, 1979). « This Paper » uses improved dark-current/blank sky corrections (see Sect. 2) which result in UV fluxes for galaxies which are larger than those listed in earlier catalogues.

TABLE II. — *NGC 224 (M 31) UV photometry.*

#	α(1950)	δ(1950)	F_λ (10^{-14} ergs cm^{-2} s^{-1} Å^{-1}) 1550	1800	2200	2500	3300	Remarks
1	00 37 39	+41 24 54	4.33±0.53	4.93±0.36	5.23±0.16	5.78±0.53	13.4±0.09	NGC 205
2	00 37 2	41 22 54	2.43±0.65	2.08±0.43	0.96±0.21	≤0.52	4.00±0.52	NGC 205
3	00 37 39	41 20 54	≤0.65	1.39±0.28	0.48±0.23	1.28±0.32	1.68±0.65	NGC 205
4	00 37 59	41 24 54	2.43±0.65	2.57±0.43	0.43±0.11	0.21±0.21	0.90±0.39	NGC 205
5	00 37 19	41 24 54	≤3.9	1.94±0.35	0.11±0.11	≤1.05	0.90±0.39	NGC 205
6	00 37 49	41 26 54	5.18±1.00	2.22±0.71	≤0.26	3.10±0.62	≤1.49	NGC 205
7	00 37 29	41 26 54	4.46±1.29	3.54±0.71	0.23±0.21	≤0.73	3.68±0.97	NGC 205
8	00 39 58	40 35 29	3.15±0.54	3.06±0.28	3.63±0.26	3.85±0.52	32.1±0.65	NGC 221
9	00 42 05	41 13 06	11.3±0.94	10.0±0.43	5.33±0.26	5.89±0.32	4.13±0.32	OB 41
10	00 41 57	41 10 06	8.72±0.53	9.03±0.56	5.33±0.26	5.67±0.63	5.88±0.78	OB 40
11	00 41 51	41 08 36	8.59±0.88	6.00±0.64	3.41±0.31	2.78±0.72	4.97±1.03	OB 39
12	00 41 13	41 01 24	5.64±0.82	5.35±0.35	2.67±0.27	2.46±0.31	5.10±0.58	OB 35
13	00 41 03	40 58 42	≤2.00	0.90±0.69	1.01±0.48	≤2.5	≤3.9	OB 34
14	00 41 42	41 04 30	7.54±0.35	7.29±0.35	3.47±0.16	3.64±0.40	3.94±0.32	OB 33
15	00 41 36	41 02 06	5.31±0.59	5.35±0.42	2.03±0.16	1.39±0.43	2.20±0.45	OB 32
16	00 41 31	41 02 24	7.41±0.82	6.18±0.57	2.93±0.21	3.00±0.31	4.20±0.39	OB 32
17	00 41 23	41 58 36	5.25±0.88	6.11±0.50	1.44±0.21	2.35±0.51	1.23±0.78	OB 31
18	00 41 14	40 58 06	3.35±1.00	2.01±1.08	2.77±0.37	≤0.94	≤1.0	OB 31
19	00 41 00	40 55 48	6.49±0.65	5.28±0.28	2.24±0.16	3.00±0.31	4.52±0.32	OB 30
20	00 40 50	40 53 42	4.66±0.94	2.22±0.57	2.13±0.21	2.57±0.51	2.71±0.58	OB 29
21	00 39 59	41 01 30	8.92±0.82	7.85±0.21	7.46±0.26	8.67±0.31	72.3±1.42	Center
22	00 40 07	41 00 12	11.2±1.89	8.61±0.56	9.01±0.47	11.1±0.94	99.6±2.07	Center
23	00 39 52	40 59 48	8.20±1.06	8.68±0.71	8.26±0.42	9.20±0.73	84.3±1.48	Center
24	00 40 01	40 58 30	9.12±0.94	6.94±0.57	6.98±0.26	9.10±0.73	73.7±1.16	Center
25	00 38 34	40 52 12	4.46±0.94	2.92±0.71	1.23±0.16	0.96±0.53	≤0.65	OB 67
26	00 38 14	40 46 48	8.33±0.65	7.43±0.57	3.15±0.16	2.78±0.51	3.29±0.58	OB 69
27	00 37 31	40 34 00	2.03±0.35	2.78±0.21	0.53±0.11	1.07±0.21	0.78±0.65	OB 72
28	00 37 38	40 33 06	3.94±1.29	2.22±0.79	1.28±0.27	2.35±0.61	≤1.2	OB 72
29	00 37 46	40 29 48	9.12±0.65	8.40±0.49	4.91±0.21	5.89±0.32	4.07±0.26	OB 78
30	00 37 53	40 28 36	14.4±1.12	11.0±0.71	7.57±0.32	6.85±0.62	5.49±0.52	OB 78
31	00 37 43	40 28 06	14.8±1.36	14.8±0.42	8.90±0.26	8.56±0.31	4.71±0.32	OB 78
32	00 37 50	40 26 54	13.7±1.00	11.7±0.78	6.45±0.26	5.99±0.53	≤1.0	OB 78
33	00 37 37	40 24 00	4.85±1.12	4.51±0.70	2.40±0.26	3.00±0.72	≤11.2	OB 79
34	00 37 32	40 22 36	5.12±0.77	3.89±0.64	2.24±0.21	1.07±0.54	0.97±0.89	OB 79
35	00 37 27	40 21 18	4.07±0.65	4.58±0.49	2.45±0.16	3.10±0.31	≤0.3	OB 79
36	00 37 42	40 20 00	8.27±0.89	8.82±0.49	4.59±0.21	3.53±0.31	2.84±0.45	OB 80
37	00 37 50	40 20 36	7.48±0.77	5.69±0.57	2.56±0.21	4.60±0.42	3.62±0.45	OB 80
38	00 37 50	40 17 36	7.48±1.35	8.26±0.85	3.09±0.31	5.14±0.84	3.23±1.03	OB 81
39	00 37 41	40 16 48	7.08±0.53	6.32±0.43	2.88±0.16	3.75±0.31	3.29±0.39	OB 81
40	00 37 48	40 15 48	8.00±0.53	7.01±0.50	3.89±0.16	3.85±0.31	1.29±0.71	OB 81
41	00 37 39	40 14 54	4.33±0.76	4.93±0.77	2.19±0.28	5.14±0.52	≤0.84	OB 81
42	00 38 10	40 18 12	3.61±0.59	5.14±0.42	2.56±0.16	2.46±0.41	3.36±0.52	OB 82
43	00 38 18	40 19 24	8.46±0.94	6.60±0.57	4.37±0.26	3.64±0.42	5.81±0.65	OB 82
44	00 38 17	40 17 24	≤0.7	3.82±0.35	1.55±0.16	≤0.7	≤6.2	OB 82
45	00 38 25	40 18 24	4.92±0.64	4.24±0.49	2.72±0.16	3.10±0.31	3.03±0.45	OB 82
46	00 36 51	40 06 24	2.89±0.58	2.36±0.43	1.12±0.16	1.71±0.32	0.7:	OB 139
47	00 40 00	40 59 24	11.9	11.3	13.7	13.6	139	Centre

TABLE III. — *NGC 598 (M 33) UV photometry.*

#	α(1950)	δ(1950)	F_λ (10^{-14} ergs cm^{-2} s^{-1} Å^{-1}) 1550	1800	2200	2500	3300	Remarks
2	01 31 41	30 42 57	4.85±0.89	4.92±0.43	2.88±0.26	3.20±0.52	8.46±0.66	
3	01 30 26	30 41 37	5.04±1.58	5.95±0.99	1.65±0.36	2.45±0.85	≤1.0	IC 132
4	01 30 27	30 37 44	14.3±1.8	11.3±1.0	6.98±0.47	7.04±0.95	≤1.2	IC 133
5	01 30 55	30 34 05	4.71±1.00	5.0±0.6	3.20±0.32	3.31±0.52	4.13±0.65	
6	01 30 39	30 32 30	6.94±1.00	7.13±0.64	3.31±0.32	4.05±0.62	2.13±0.71	
7	01 30 25	30 30 14	13.8±2.0	10.8±0.78	6.13±0.21	5.23±0.31	4.52±0.90	IC 131
8	01 30 17	30 27 23	6.35±0.64	5.26±1.35	2.88±0.63	2.45±2.45	≤1.9	
9	01 29 54	30 23 38	9.04±0.65	5.68±0.36	4.48±0.26	3.20±0.21	≤2.1	NGC 588
10	01 30 07	30 23 38	9.89±1.30	7.48±0.71	5.17±0.37	2.67±0.51	4.39±1.23	
11	01 30 21	30 23 38	11.7±1.30	11.1±1.48	6.51±0.78	6.83±1.16	1.42±0.97	NGC 592
12	01 30 20	30 21 15	2.55±1.19	4.08±0.28	1.71±0.16	1.07±1.00	≤1.6	
13	01 30 07	30 20 41	22.8±1.8	17.6±0.9	14.9±0.6	10.1±0.8	2.32±0.71	
14	01 30 20	30 18 52	17.9±1.2	13.5±0.6	8.96±0.31	8.00±0.53	5.49±0.78	
15	01 30 31	30 18 52	---	---	---	---	---	Not Obs
16	01 30 31	30 16 02	11.4±1.6	11.5±0.71	7.41±0.37	9.07±0.63	7.43±0.65	
17	01 30 20	30 12 05	9.56±0.77	7.13±0.78	3.52±0.42	3.84±0.43	2.78±0.97	
18	01 29 47	30 09 19	1.3:	1.87±0.72	2.35±0.37	1.1:	≤9.2:	
19	01 30 48	30 07 59	23.6±1.4	105±2	107±1	96.1±1.9	135±2	
20	01 31 14	30 11 29	5.11±1.00	4.29±0.49	2.83±0.31	2.88±0.51	2.71±0.65	
21	01 30 52	30 12 48	7.14±1.06	5.82±0.57	3.31±0.32	4.80±0.52	4.33±0.58	
22	01 30 40	30 16 02	11.8±1.6	10.5±1.1	7.14±0.53	7.04±1.16	3.68±2.26	
23	01 30 54	30 17 33	28.4±1.8	22.2±1.2	15.6±1.1	14.4±0.14	9.68±1.23	
24	01 31 07	30 18 25	38.6±2.4	32.1±1.2	23.7±0.7	21.0±0.9	15.4±0.84	IK 44
25	01 31 27	30 18 31	21.9±1.6	17.1±0.9	11.8±0.5	12.0±0.7	8.14±0.65	
26	01 31 24	30 21 15	22.4±1.8	18.8±1.2	12.4±0.6	18.9±1.0	5.04±0.9	
27	01 31 12	30 21 15	29.1±2.3	26.4±2.1	16.0±0.6	14.3±1.2	13.1±1.2	
28	01 31 00	30 21 15	21.5±1.7	17.4±1.0	11.9±0.5	11.4±0.8	11.0±1.0	
29	01 30 50	30 21 15	29.4±1.8	25.5±1.6	15.9±1.4	18.4±1.5	11.1±1.8	IK 25
30	01 30 50	30 23 45	23.4±0.6	20.4±0.7	14.0±1.3	13.3±0.4	12.7±0.9	
31	01 31 04	30 23 53	44.0±3.0	42.8±1.7	31.0±1.4	28.8±1.6	30.3±1.3	Centre
32	01 31 12	30 23 45	28.4±2.2	27.5±1.4	18.7±0.7	17.4±1.2	16.5±1.2	
33	01 31 24	30 24 19	19.5±1.5	16.4±0.9	11.4±0.5	9.82±0.73	8.46±0.65	
34	01 30 39	30 25 19	13.2±1.6	12.4±0.6	7.19±0.42	7.58±0.42	6.13±0.65	NGC 595
35	01 30 50	30 26 15	19.7±2.0	16.1±1.0	11.0±0.5	11.1±1.9	15.6±1.1	
36	01 31 00	30 26 15	18.5±1.5	14.1±0.8	10.1±0.5	9.9±0.7	12.7±0.8	
37	01 31 10	30 26 15	13.3±1.6	16.1±1.0	9.44±0.47	8.22±0.82	11.0±1.0	
38	01 30 50	30 28 45	10.6±1.2	9.35±0.61	5.81±0.37	6.08±0.63	6.52±0.65	IK 30
39	01 31 06	30 30 23	14.5±1.4	13.2±0.9	8.21±0.42	8.11±0.74	9.17±0.71	IC 142
40	01 31 16	30 32 08	17.9±1.5	17.5±0.9	10.8±0.5	12.4±0.7	9.88±0.71	IK 53
41	01 31 31	30 33 40	9.82±1.23	7.06±0.71	4.11±0.21	4.05±1.66	6.39±0.71	
42	01 31 40	30 31 40	50.1±2.9	44.1±2.8	30.3±1.0	25.3±2.0	19.3±1.0	NGC 604
43	01 31 47	30 28 48	15.7±1.9	11.2±1.1	7.14±0.46	6.08±0.94	7.17±1.10	
44	01 31 51	30 26 25	9.04±1.12	8.59±0.57	4.59±0.32	4.69±0.52	1.55±0.58	
45	01 31 31	30 27 16	4.58±1.17	5.12±1.01	2.67±0.31	2.56±1.54	≤0.8	
46	01 28 40	30 40 00	2.29±1.00	4.85±0.50	0.69±0.21	≤1.1	≤1.9	
47	01 32 00	29 50 00	2.95±0.77	2.15±0.65	≤0.3	≤0.7	1.03±0.97	

TABLE IV. — *NGC 3031 (M 81) UV photometry.*

#	α(1950)	δ(1950)	F_λ (10^{-14} ergs cm^{-2} s^{-1} Å^{-1}). 1550	1800	2200	2500	3300	Remarks
1	09 52 38	+69 10 37	2.23±0.76	1.03±0.41	0.15±0.15	2.56±0.41	15.5±6.9	
2	09 52 10	69 10 37	5.49±2.89	2.76±0.57	1.58±0.53	5.34±2.09	13.6±2.2	
3	09 51 42	69 10 37	2.13±1.48	1.72±0.51	0.77±0.10	≤0.7	≤1.4	
4	09 51 14	69 10 37	2.60±1.54	2.20±0.99	≤0.4	≤1.1	1.10±0.58	
5	09 52 24	69 13 07	3.86±1.54	2.48±0.43	0.87±0.36	2.03±0.75	≤1.8	
6	09 51 56	69 13 07	8.45±1.94	6.54±1.00	3.78±0.47	4.27±0.73	3.42±2.17	
7	09 51 28	69 13 07	2.45±2.45	2.48±0.78	1.33±0.33	2.03±1.00	≤3.0	
8	09 51 00	69 13 07	1.79±1.25	≤1.8	1.07±0.32	1.39±1.39	1.55±1.50	
9	09 52 38	69 15 37	6.42±2.07	3.79±1.54	1.58±0.79	6.19±2.31	10.9±1.16	
10	09 52 10	69 15 37	3.91±1.78	4.75±2.13	2.45±0.73	2.88±0.41	≤1.0	
11	09 51 42	69 15 37	≤2.1	1.10±0.96	1.74±0.48	≤1.8	11.0±4.2	
12	09 51 14	69 15 37	≤2.2	1.31±1.17	0.87±0.31	0.85±0.32	2.00±0.45	
13	09 50 46	69 15 37	2.12±1.12	2.96±0.83	0.92±0.56	≤1.8	≤1.7	
14	09 52 24	69 18 07	5.42±1.41	3.24±1.48	1.99±0.31	2.14±1.07	≤5.7	
15	09 51 56	69 18 07	3.05±1.94	2.34±1.35	1.79±0.47	2.03±1.60	≤2.6	
16	09 51 28	69 18 07	---	---	---	---	---	
17	09 51 00	69 18 07	2.12±1.06	1.24±0.96	0.92±0.20	≤1.2	≤4.8	
18	09 50 32	69 18 07	5.04±1.00	3.58±1.19	1.89±0.63	2.46±0.41	≤1.9	
19	09 52 10	69 20 37	6.23±1.23	4.82±1.78	2.09±0.63	2.46±1.13	2.52±1.94	
20	09 51 42	69 20 37	1.59±1.59	2.07±2.07	1.02±0.36	≤2.4	3.49±2.00	
21	09 51 14	69 20 37	≤2.3	2.96±0.74	1.48±0.58	2.67±1.95	6.39±1.61	
22	09 50 46	69 20 37	5.50±1.56	5.24±1.98	2.60±0.73	4.06±1.87	6.97±4.13	
23	09 50 18	69 20 37	1.33±0.75	2.07±1.64	≤0.8	3.20±3.20	≤2.3	
24	09 51 56	69 23 07	2.65±1.30	2.07±0.93	1.28±0.21	1.71±0.64	≤1.8	
25	09 51 28	69 23 07	4.97±1.23	3.44±1.19	2.50±0.52	2.88±1.23	2.65±1.94	
26	09 51 00	69 23 07	7.49±1.59	7.09±0.64	3.27±0.21	4.81±0.42	5.62±1.61	
27	09 50 32	69 23 07	2.52±1.70	2.14±1.07	0.87±0.46	1.28±1.07	≤2.1	
28	09 51 42	69 25 37	3.32±1.30	2.41±1.06	0.61±0.10	1.07±1.07	≤9.5	
29	09 51 14	69 25 37	3.38±1.66	2.69±0.64	1.07±0.04	2.14±0.43	≤3.1	
30	09 50 46	69 25 37	≤1.1	2.76±1.91	0.87±0.67	≤1.9	≤3.9	
31	09 50 18	69 25 37	2.52±2.29	2.14±1.50	0.97±0.77	3.20±2.06	≤2.8	
32	09 51 30	69 19 01	1.83±1.06	2.62±0.92	2.17±0.47	2.96±0.61	34.5±1.6	Centre

TABLE V. — *NGC 5457 (M 101) UV photometry.*

#	α(1950)	δ(1950)	F_λ (10^{-14} ergs cm^{-2} s^{-1} Å^{-1}). 1550	1800	2200	2500	3300	Remarks
2	14 00 00	+54 27 06	≤3.2	≤1.3	≤0.8	≤2.3	≤4.8	
3	14 00 42	54 35 35	9.0±1.7	9.5±1.5	5.4±0.5	8.6±1.1	---	
4	14 00 43	54 30 41	11.7±1.4	12.5±1.6	7.5±0.5	5.5±1.1	4.2±2.6	NGC5447
5	14 00 51	54 30 14	10.2±1.8	7.9±0.8	4.7±1.2	4.3±1.1	---	NGC5447
6	14 01 04	54 29 44	9.0±1.9	7.7±2.4	5.8±0.4	2.2±1.9	≤4.0	NGC5455
7	14 01 31	54 30 00	9.5±3.2	8.6±0.9	3.2±0.8	6.9±1.1	10.7±1.1	
8	14 01 32	54 36 21	9.0±1.4	11.3±2.3	7.3±0.8	8.2±1.6	6.9±3.5	#20
9	14 01 38	54 34 08	21.4±2.4	20.0±2.9	11.2±1.8	14.6±3.5	≤7.2	S4
10	14 01 40	54 33 25	10.9±2.5	13.8±1.1	8.8±0.9	5.6±1.3	5.5±5.0	
11	14 01 55	54 33 27	16.7±4.2	17.3±2.5	8.0±0.5	10.5±1.1	14.7±1.8	NGC5461
12	14 01 57	54 43 52	≤1.7	4.7±0.7	1.6±0.5	3.6±1.2	2.3:	
13	14 02 01	54 34 52	7.4±3.4	6.9±1.8	4.0±0.7	3.9±2.6	3.8±1.0	
14	14 02 07	54 36 20	14.5±1.5	12.5±0.8	8.0±0.5	6.2±2.0	≤6.7	NGC5462
15	14 02 18	54 35 00	6.7±2.2	4.6±1.8	2.1±0.8	3.5±1.4	3.9±1.7	
16	14 02 25	54 38 09	12.0±3.7	11.0±4.5	4.5±0.7	7.9±2.1	---	
17	14 02 44	54 38 09	14.4±2.0	10.5±2.4	5.9±1.3	5.5±1.1	≤3.5	NGC5471
18	14 03 32	54 55 00	≤2.8	3.8±2.4	≤0.7	2.5±1.8	≤3.3	
19	14 04 04	54 52 56	≤1.7	≤1.2	≤0.6	≤0.7	---	

TABLE VI. — *NGC 2403 UV photometry.*

#	α(1950)	δ(1950)	F_λ (10^{-14} ergs cm^{-2} s^{-1} Å^{-1}). 1550	1800	2200	2500	3300	Remarks.
1	07 32 06	+65 42 42	26.3	28.1	18.7	17.5	21.3	Centre
2	07 32 19	+65 43 12	17.0±2.9	17.7±4.2	13.3±0.9	13.2±2.3	≤38.9	VS 44
3	07 32 11	+65 44 06	18.5±0.2	20.5±0.9	12.4±0.5	11.6±1.0	≤46.0	VS 41

TABLE VII. — *Photometry of compact (Zwicky) galaxies.*

#[a]	α(1950)	δ(1950)	F_λ (10^{-14} ergs cm^{-2} s^{-1} Å^{-1}). 1550	1800	2200	2500	3300	Remarks.
30	04 31.6	-08 41	≤3.3	≤2.5	≤0.9	≤2.1	≤7.6	IIZw15
40	05 53.1	+03 24	≤0.8	≤0.9	≤0.4	≤0.7	≤1.4	IIZw40
41	06 00.4	07 50	≤1.7	≤1.1	≤0.4	≤1.6	≤1.7	IIZw42
42	08 24.3	55 52	≤2.0	≤1.3	≤0.6	≤1.3	≤3.3	IZw14
43	08 24.8	21 39	3.0±2.0	2.5±1.0	1.5±0.5	1.4±0.7	4.0±1.0	IIIZw59
44	09 01.0	55 43	≤2.1	≤1.8	≤1.0	≤3.1	≤1.9	IZw17
--	09 30.5	55 27	1.6±1.0	≤1.3	0.6±0.4	≤1.5	≤2.0	IZw18
47	09 43.3	45 59	≤2.1	≤1.4	≤0.8	≤1.6	≤4.6	IZw21
48	09 56.0	52 29	≤1.6	≤1.8	≤0.6	≤1.5	≤2.9	IZw23
--	10 00.4	59 41	≤3.0	≤4.0	0.7±0.4	≤2.8	≤2.3	VIIZw308
49	10 12.5	21 20	≤1.6	≤0.8	≤0.5	≤0.7	≤2.6	IIZw44
50	10 18.5	28 11	≤1.4	≤0.9	≤0.4	≤1.0	≤2.1	IZw24
51	10 25.1	22 00	≤1.5	≤2.0	≤1.4	≤1.4	≤3.2	IIZw46
52	10 25.2	19 45	2.6±1.0	≤1.0	0.7±0.3	1.2±0.6	1.4±0.9	IIZw47
55	11 36.3	45 53	2.0±1.2	≤0.7	≤0.4	≤1.1	≤1.5	IIZw53
--	12 54.1	57 09	≤1.5	0.9±0.6	0.4±0.3	≤1.0	≤1.6	VIIZw490
--	13 21.5	70 47	4.9±0.7	5.0±0.5	3.7±0.2	3.0±0.4	2.5±0.5	VIIZw511
--	13 42.9	56 08	≤3.0	≤1.9	≤1.3	≤1.7	≤3.3	IZw71
102	17 39.0	47 46	≤3.0	≤2.2	≤0.7	≤2.1	≤4.0	IZw191
104	17 49.3	56 41	≤2.7	≤2.4	≤0.8	≤2.0	≤3.6	IZw199
105	17 50.6	54 00	≤1.8	≤1.6	≤0.4	≤1.0	≤3.3	IZw201
106	18 24.9	34 18	≤2.8	≤2.1	≤0.5	≤1.7	≤27.0	IZw206
107	18 30.2	55 14	≤2.0	≤1.8	≤0.7	≤1.9	≤4.0	IZw207
108	18 31.6	54 29	≤3.0	≤1.8	≤1.1	≤1.9	≤3.3	IZw208
112	21 39.7	25 04	≤1.5	≤1.0	≤0.5	≤1.2	≤1.4	IVZw74
113	22 07.2	17 24	≤1.3	≤1.2	≤0.5	≤1.1	≤1.8	
--	23 18.0	16 57	1.8±1.2	≤1.9	≤1.3	≤1.7	≤3.3	IIIZw103

Note to table VII: a. Number given refers to Sargent (1970). Note that Sargent's IZw numbers should be increased by one.

TABLE VIII. — *Radial distribution of UV emission in M 33.*

$F_\lambda(R) = F_\lambda(0) \times e^{-aR}$ erg cm^{-2} s^{-1} Å^{-1} (R in arcmin).

Wavelength	$F_\lambda(0)$	a	Correl. Coeff. r	Number n	'Bulge Excess' F_λ (Bulge)
1550	2.58 10^{-13}	0.060	0.59	41	2.32 10^{-13}
1800	2.40	0.066	0.64	42	1.90
2200	1.64	0.070	0.69	41	1.53
2500	1.90	0.087	0.72	42	1.07
3300	1.72	0.100	0.77	41	1.31

TABLE IX. — *Radial distribution of UV emission in M 101.*

$F_\lambda(R) = F_\lambda(0) \times e^{-aR}$ erg cm^{-2} s^{-1} Å^{-1} (R in arcmin).

Wavelength λ	$F_\lambda(0)$	a	Correl. Coeff. r	Number n
1550	1.46 10^{-13}	0.063	0.32	15
1800	1.51	0.067	0.47	15
2200	0.95	0.093	0.50	15
2500	0.92	0.072	0.44	15
3300	0.96	0.097	0.58	12

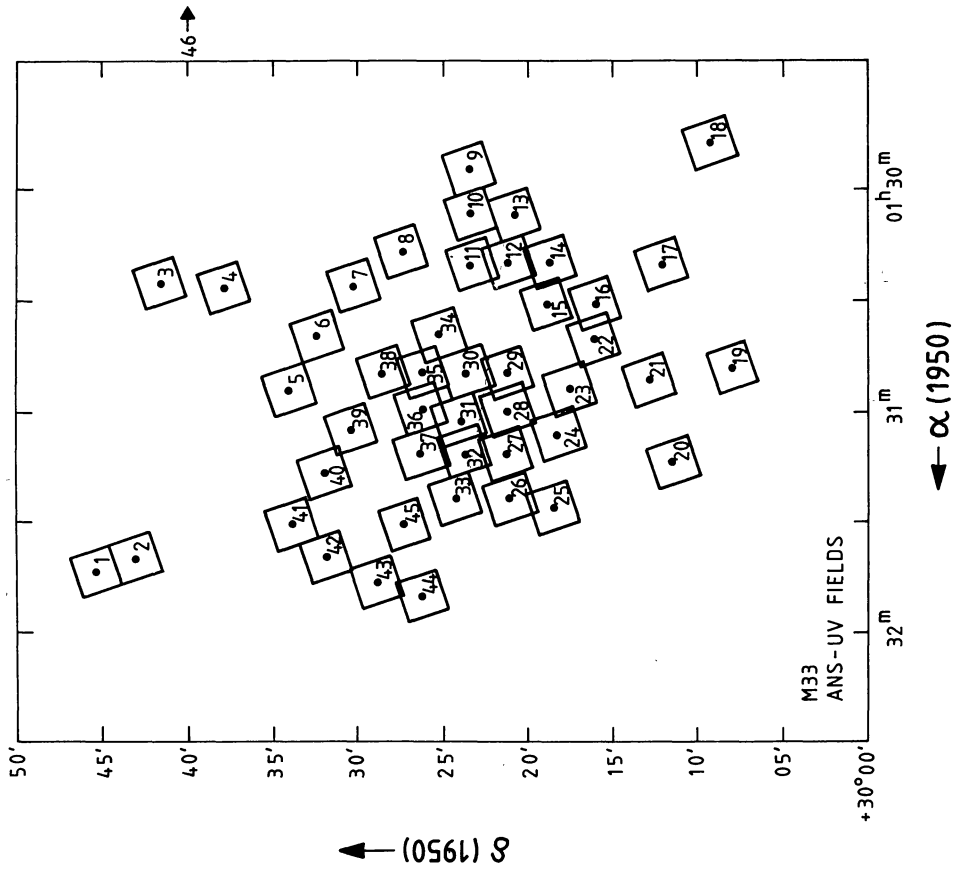

FIGURE 2. — ANS coverage of M 33. The numbers refer to table III.

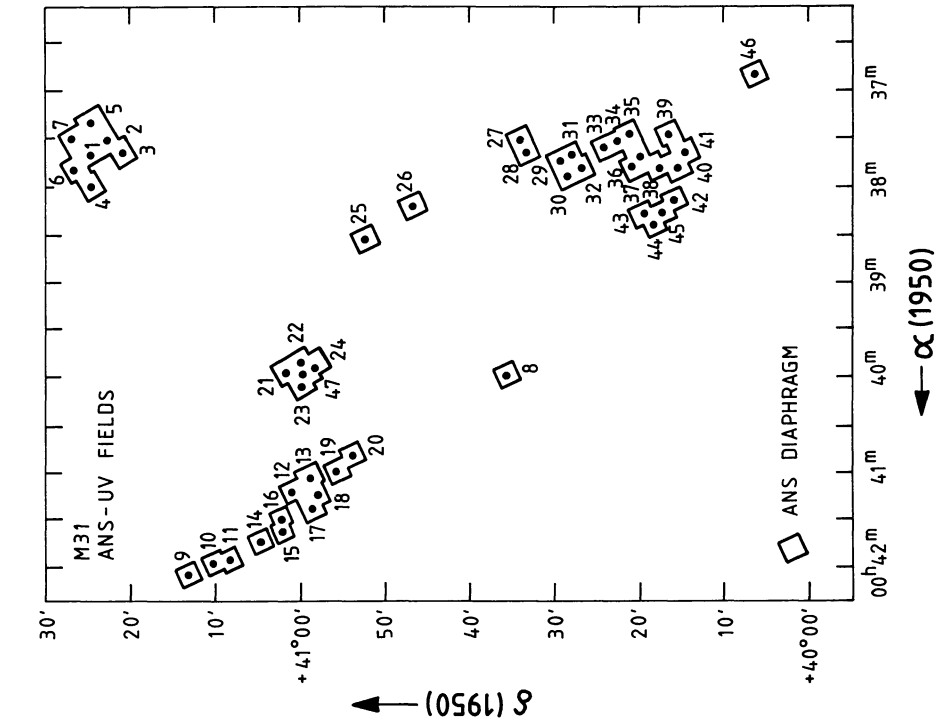

FIGURE 1. — ANS coverage of M 31. The numbers refer to table II.

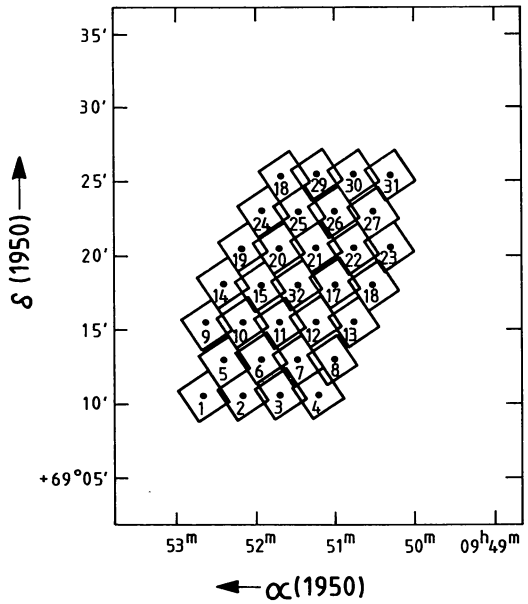

FIGURE 3. — ANS coverage of M 81. The numbers refer to table IV.

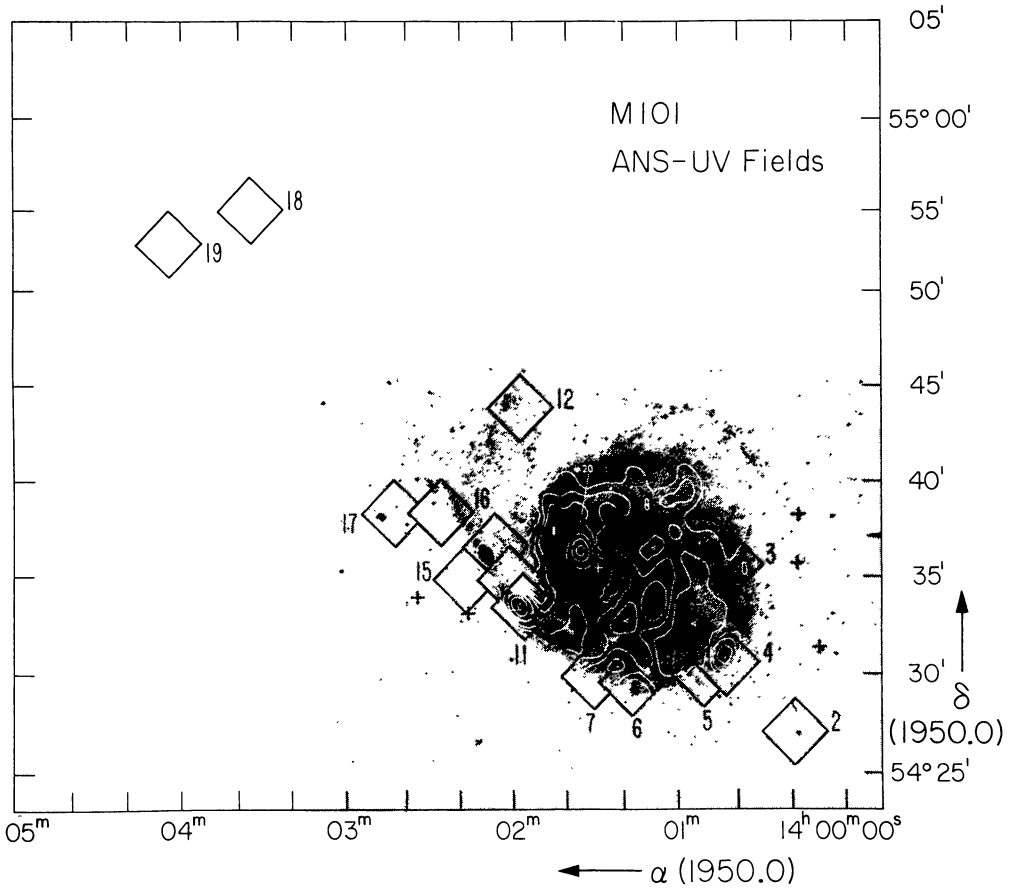

FIGURE 4. — ANS coverage of M 101. The numbers refer to table V.

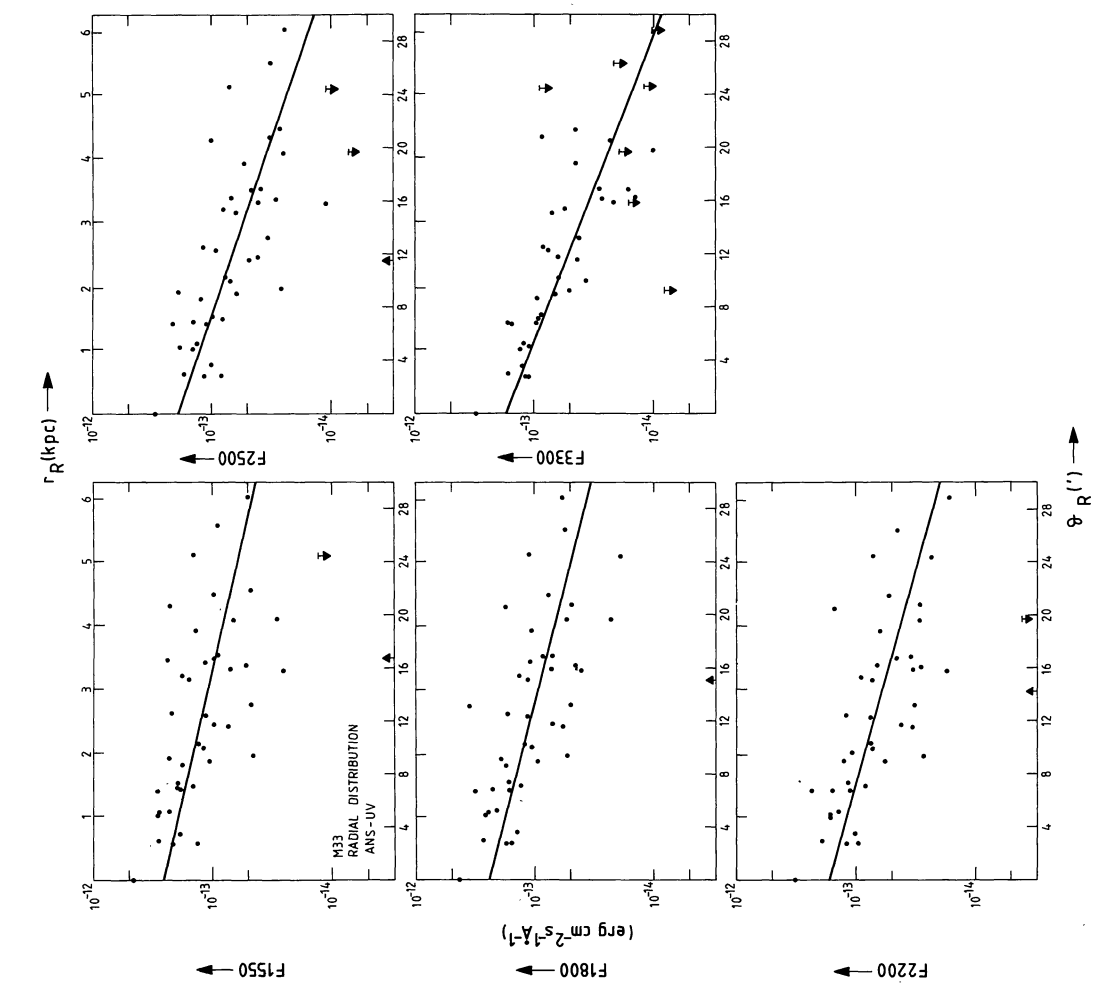

FIGURE 6. — Radial distribution of UV intensities over the disk of M 33 in the five ANS bands.

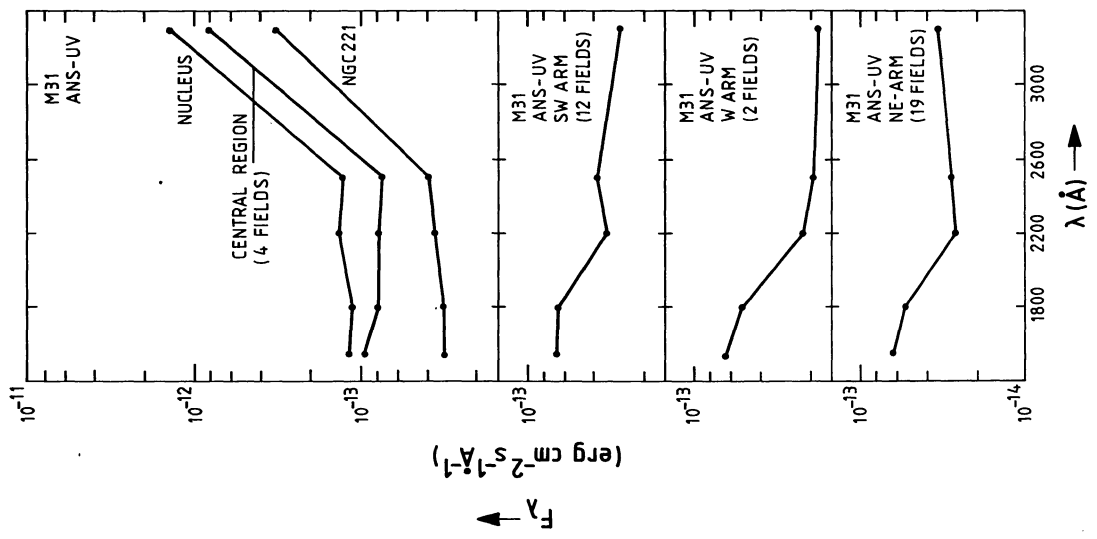

FIGURE 5. — Averaged ANS-UV spectra for four groups of fields in M 31.

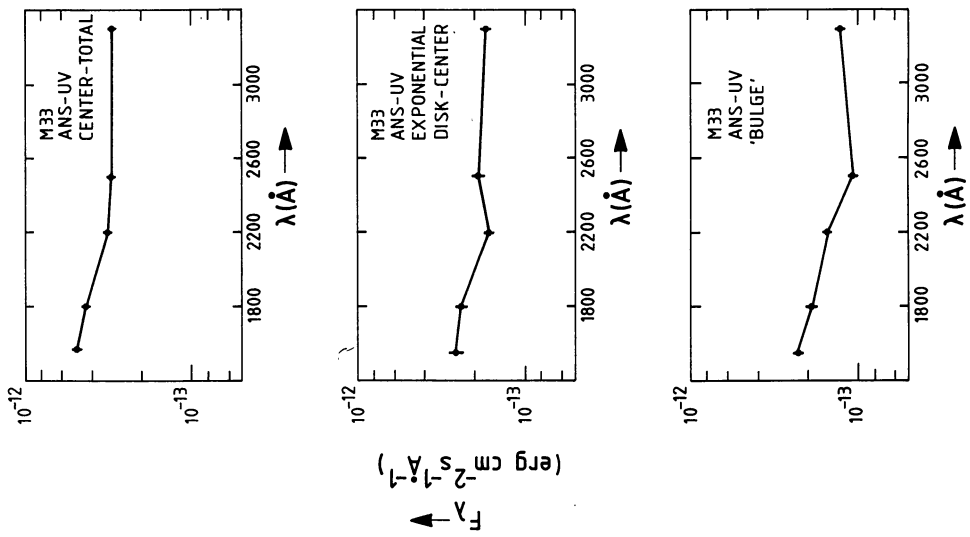

FIGURE 7. — UV spectrum of the central 2.5 arcmin region of M 33 decomposed into extrapolated disk and a bulge « excess » contributions.

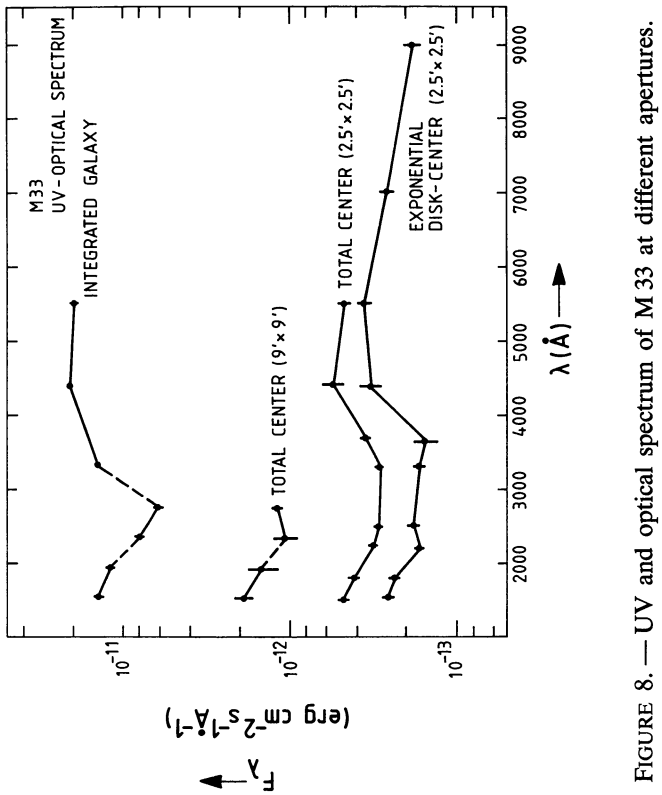

FIGURE 8. — UV and optical spectrum of M 33 at different apertures.

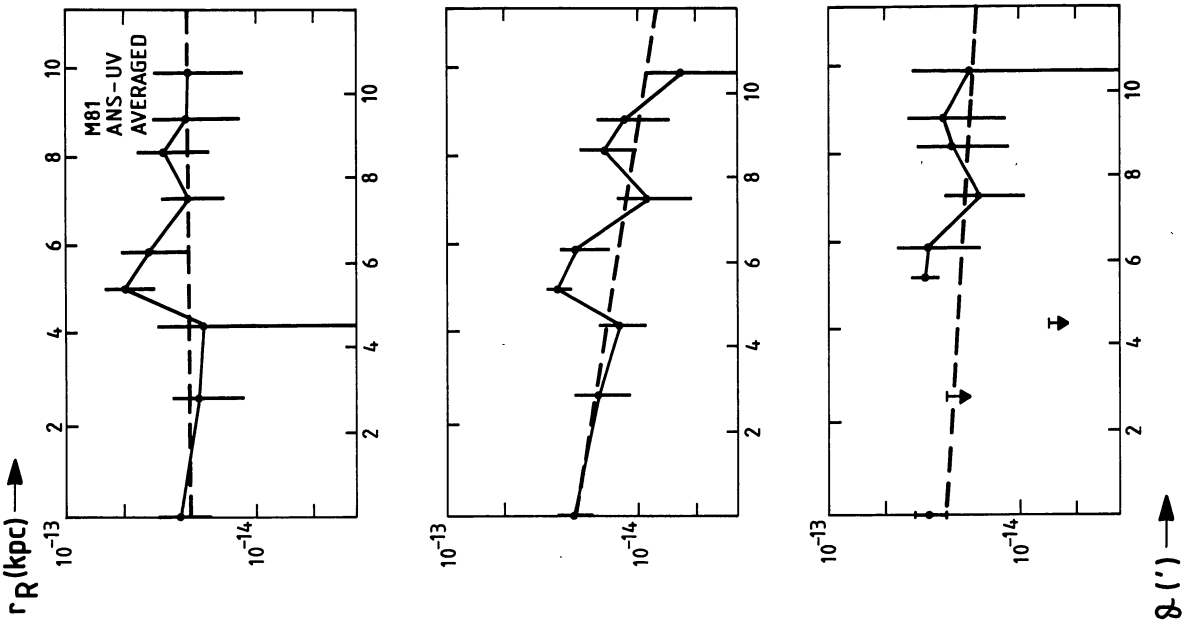

FIGURE 10. — Same as figure 9, but now the data have been smoothed over one arcmin bins.

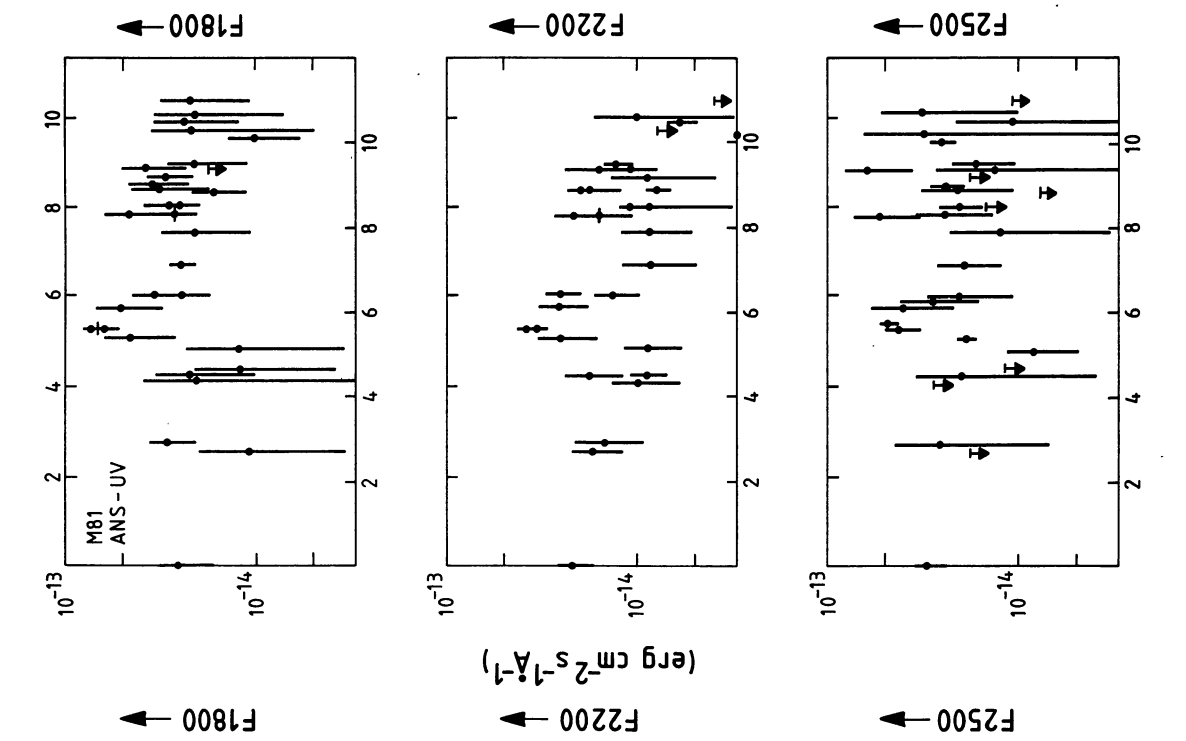

FIGURE 9. — Radial distribution of UV intensities over the disk of M 81 in 1800, 2200 and 2500 Ångström bands.

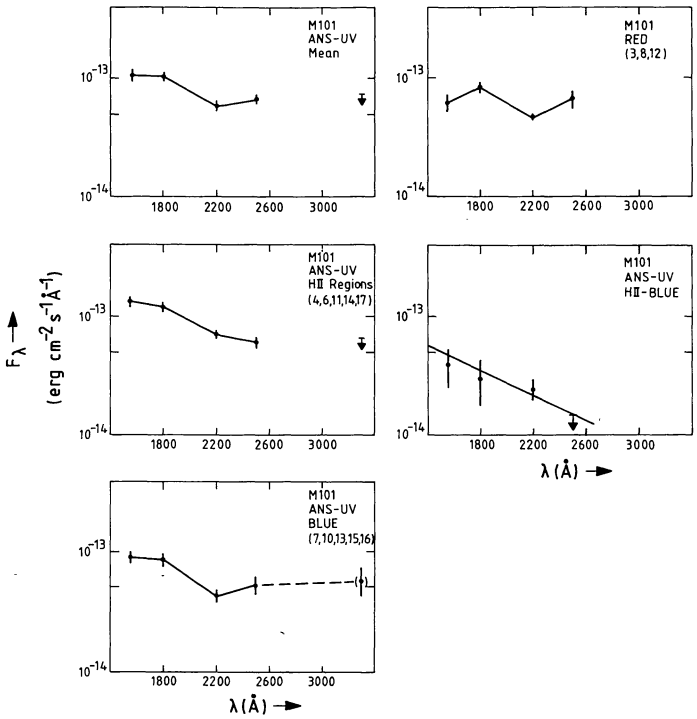

FIGURE 11. — ANS-UV spectra of different groups of fields in M 101. See text.

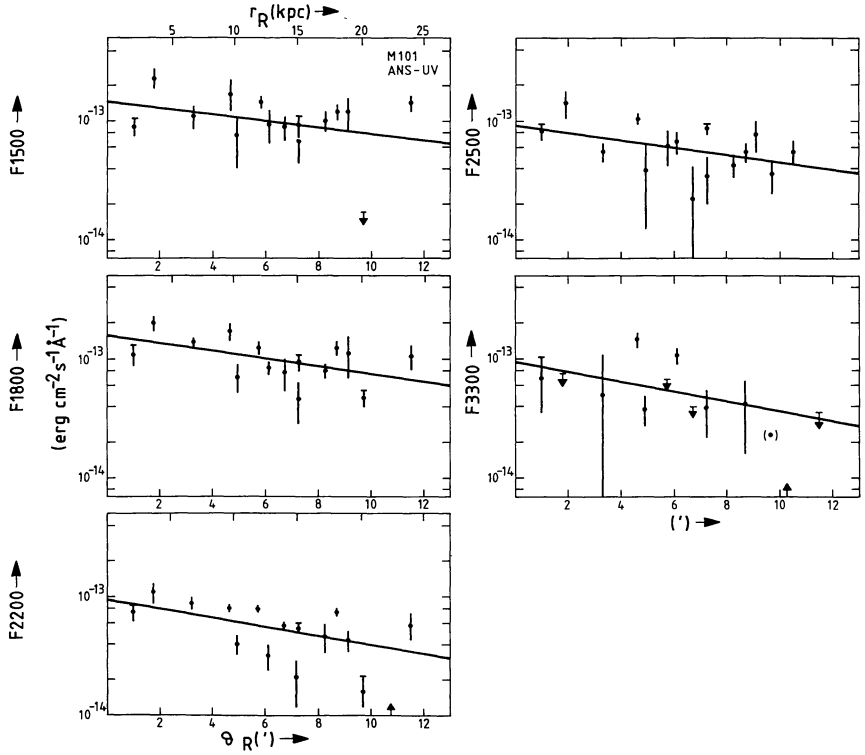

FIGURE 12. — Radial distribution of UV intensities over the disk of M 101 in the five ANS bands.